Cell, Vol. 90, 537–548, August 8, 1997, Copyright ©1997 by Cell Press

Formation of Neuronal Intranuclear Inclusions Underlies the Neurological Dysfunction in Mice Transgenic for the HD Mutation

Stephen W. Davies,* Mark Turmaine,*
Barbara A. Cozens,* Marian DiFiglia,†
Alan H. Sharp,‡ Christopher A. Ross,‡
Eberhard Scherzinger,§ Erich E. Wanker,§
Laura Mangiarini,‖ and Gillian P. Bates‖
*Department of Anatomy and Developmental Biology
University College London
Gower Street
London WC1E 6BT
United Kingdom
†Department of Neurology
Massachusetts General Hospital
Harvard Medical School
Boston, Massachusetts 02114
‡Department of Psychiatry and Behavioral Sciences
Johns Hopkins University
Baltimore, Maryland 21205-2183
§Max Planck Institut für Molekulare Genetik
Berlin (Dahlem), Germany
‖Division of Medical and Molecular Genetics
UMDS, Guy's Hospital
London SE1 9RT
United Kingdom

Summary

Huntington's disease (HD) is one of an increasing number of human neurodegenerative disorders caused by a CAG/polyglutamine-repeat expansion. The mutation occurs in a gene of unknown function that is expressed in a wide range of tissues. The molecular mechanism responsible for the delayed onset, selective pattern of neuropathology, and cell death observed in HD has not been described. We have observed that mice transgenic for exon 1 of the human *HD* gene carrying $(CAG)_{115}$ to $(CAG)_{156}$ repeat expansions develop pronounced neuronal intranuclear inclusions, containing the proteins huntingtin and ubiquitin, prior to developing a neurological phenotype. The appearance in transgenic mice of these inclusions, followed by characteristic morphological change within neuronal nuclei, is strikingly similar to nuclear abnormalities observed in biopsy material from HD patients.

Introduction

Huntington's disease (HD) is an autosomal dominant progressive neurodegenerative disorder (Harper, 1991). Onset is generally in midlife but can vary from early childhood until well into old age, and the disease duration is generally 15 to 20 years. The disorder is characterized by a complex and variable set of symptoms that have psychological, motor, and cognitive components. The motor component of the adult form of the disease can include chorea, dystonia, dysarthria, dysphagia, and restlessness; however, the disorder may progress to an akinetic state. The juvenile form generally presents with a Parkinsonian rigidity and in some cases chorea may never be seen. Juvenile symptoms also include myoclonus, epileptic seizures, and tremor. Patients have a very high calorific intake but paradoxically generally lose weight. Currently, HD has no effective therapy.

The most thorough study of the neuropathology of HD classified the neuropathological changes into five grades: grade 0, in which HD brains show no gross or generalized microscopic abnormalities consistent with HD, despite premortem symptomatology and positive family history, progressing to grade 4, in which the most extreme atrophy is observed (Vonsattel et al., 1985). All grades exhibit a 30% reduction in the weight of HD brains, which has been shown to be associated with 20% to 30% areal reductions in cerebral cortex, white matter, hippocampus, amygdala, and thalamus (de la Monte et al., 1988). This suggests that the shrinkage of these structures occurs early in the disease process and is not progressive. Gliosis was not readily apparent in these structures and the neuronal density was assessed to be normal (de la Monte et al., 1988). In contrast, the progressive reduction in the cross-sectional area of the caudate, putamen, and globus pallidus increases to 60% in grades 3 to 4 HD brains, indicating that these structures progressively degenerate with prolonged survival. This specific progressive atrophy is associated with reactive astrocytosis (Vonsattel et al., 1985; Myers et al., 1991). Studies by Hedreen and Folstein (1995) suggest that grade 0 brains, while displaying no generalized striatal pathology, do have scattered islands of reactive astrocytes and circumscribed neuronal cell loss that correspond to the striosomal compartments of the striatum. These are the earliest pathological changes so far reported in HD and were found in individuals who had a 3- to 5-year history of chorea, although grade 0 pathology has been observed after up to 13 years of chorea (Vonsattel et al., 1985; Myers et al., 1988).

The mutation underlying HD has been identified as a CAG/polyglutamine (polygln) expansion in the first exon of a gene encoding a large 350 kDa protein of unknown function (Huntingtons Disease Collaborative Research Group, 1993). The CAG repeat sizes in the normal and expanded ranges are $(CAG)_6$ to $(CAG)_{39}$ and $(CAG)_{35}$ to $(CAG)_{180}$ (referenced in Bates et al., 1997). The vast majority of adult onset cases have expansions ranging from 40 to 55 units; expansions of 70 and above invariably cause the juvenile form of the disease, and very few cases have been described with expansions above 100. The expression profile of huntingtin (htt) does not account for the characteristic pattern of neuropathology observed in the brains of HD patients. Huntingtin has been identified in all peripheral tissues studied and within the brain is found to be predominently neuronal with no enrichment in the basal ganglia. It is present in cell bodies and dendrites and appears enriched in neuronal terminals, possibly associated with synaptic vesicles or microtubules (DiFiglia et al., 1995; Gutekunst et al., 1995; Sharp et al., 1995; Trottier et al., 1995a). At the ultrastructural level, immunoreactivity in cortical neurons was detected in the matrix of the cytoplasm

and around the membrane of synaptic vesicles (DiFiglia et al., 1995; Gutekunst et al., 1995).

The dominant mechanism by which the polygln expansion causes neurodegenerative disease is unknown. The mutation does not shut down transcription or translation of the *HD* gene (Ide et al., 1995; Jou and Myers, 1995; Schilling et al., 1995; Trottier et al., 1995a), as mutant htt can be detected on Western blots of protein isolated from both brain and peripheral tissues. In addition, a dominant negative pathway has been ruled out by the generation of mouse knockouts in which the nullizygous mice have an embryonic lethal phenotype (Duyao et al., 1995; Nasir et al., 1995; Zeitlin et al., 1995). A gain-of-function mechanism has been supported by the identification of an antibody that specifically detects pathogenic polygln expansions (Trottier et al., 1995b), suggestive of a change in conformation occurring upon a certain size threshold, possibly facilitating novel interactions. However, the molecular events by which a polygln expansion causes cell death remain to be unraveled.

CAG/polygln expansion has been found to form the molecular basis for seven neurodegenerative disorders. In addition to HD, the mutated gene has been identified for spinal and bulbar muscular atrophy (SBMA), dentatorubral pallidoluysian atrophy (DRPLA), and spinocerebellar ataxia (SCA) types 1, 2, 3, and 6 (referenced in Bates et al., 1997). The normal and expanded repeat ranges are broadly comparable, suggesting a pathogenic threshold in the length of the polygln tract occurring at approximately 37 to 40 residues. It is likely that a similar gain-of-function mechanism is applicable to all of these diseases (except in the case of SCA6, for which the expanded alleles are smaller and the mutation is likely to act by a different route). The proteins harboring the polygln stretches are mostly novel and otherwise unrelated but in all cases are widely or ubiquitously expressed. Despite extensively overlapping expression patterns, the neuronal cell death is relatively specific and can differ markedly (Ross, 1995), although in the juvenile forms of these diseases the neuropathology becomes more widespread and less distinct. The factors that convey the specific patterns of neurodegeneration are not understood.

We have recently generated lines of mice (R6) that are transgenic for the HD mutation (Mangiarini et al., 1996). The transgene contains ~1 kb of the human HD promoter region, exon 1 carrying CAG-repeat expansions of 115 to 156 units, and 262 bp of intron 1. Three lines, R6/1, $(CAG)_{115}$; R6/2, $(CAG)_{145}$; and R6/5, $(CAG)_{128–156}$, develop a progressive neurological phenotype. A phenotype has not been observed in a fourth line (R6/0) in which the transgene is not expressed nor in two further lines transgenic for the same construct carrying 18 repeats (HDex6 and HDex27). Line R6/2 has been characterized most extensively. The mice carry repeat expansions ranging from 141 to 157 repeats, the variability having arisen from germ line instability (Mangiarini et al., 1997). They exhibit a progressive, complex neurological phenotype with an age of onset of approximately 2 months. The progression of the disease is rapid and the mice deteriorate over the following month. The movement disorder includes a resting tremor, rapid, abrupt shuddering movements, stereotypic grooming movements, and epileptic seizures. The body weight of the R6/2 males decreases steadily from 8 weeks, such that at 12 weeks transgenic males weigh approximately 60% of littermate controls. The R6/2 mice are reproductively compromised and show urinary incontinence, of which the cause, as in HD patients, is unknown. The mice appear to model many features of HD, particularly those of the juvenile variant. At 12 weeks, the only difference between the transgenes and controls on neuropathological analysis was that the brains weighed ~20% less than the normal littermate controls. The reduction in size was constant throughout all CNS structures, which had an apparently normal neuronal density.

In this report, we have extended the neuropathological study to include immunocytochemical analysis with a number of antibodies raised against the N terminus of the htt protein. In transgenic mice prior to the onset of symptoms and in control mice, the transgene shows a diffuse cytoplasmic staining as previously reported for htt in rat, primate, and human brain (DiFiglia et al., 1995; Gutekunst et al., 1995; Sharp et al., 1995; Trottier et al., 1995a). We have identified a nuclear localization of the transgene protein that correlates with symptomatology in each of the R6/1, R6/2, and R6/5 lines. At the ultrastructural level, this appears as a neuronal intranuclear inclusion (NII), and associated nuclear changes include invaginations of the nuclear membrane and an increase in the nuclear pore density.

Results

Transgene Expression in the R6 and HDex Lines

Expression analysis of the R6 transgenes using RT-PCR and Northern and Western analysis was described in our initial report (Mangiarini et al., 1996). Lines R6/1, R6/2, and R6/5 showed ubiquitous expression by RT-PCR in a panel of 18 brain regions and somatic tissues, and a transcript was detected on a Northern blot for each of these lines. Western analysis was carried out using the 1C2 antibody (Trottier et al., 1995b), which specifically recognizes pathogenic polygln expansions. Using this antibody we initially did not detect a protein product in line R6/1, although the transgene protein was readily detectable in lines R6/2 and R6/5. As all three of these lines develop a phenotype, one possible interpretation of this result is that the mutation is acting at the RNA rather than the protein level. However, we have since been able to detect the transgene protein in line R6/1 using three different N-terminal antibodies: AB78, HD1, and CAG53b, illustrated in Figure 1. The size difference observed in the transgene proteins corresponds to the length of the polygln tract. As previously described, proteins containing polyglns migrate comparatively slowly through SDS-PAGE gels (Aronin et al., 1995). We can now also demonstrate the presence of the transgene protein product in the HDex control lines (18 CAG repeats), and it is clear that a much lower level of expression is present in line HDex6 as compared to the other lines. No evidence of expression at the RNA or protein level was detected in line R6/0.

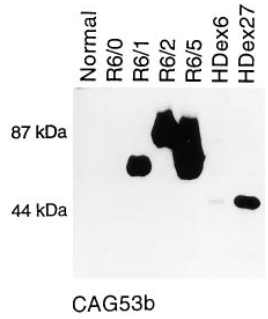

Figure 1. Expression of the Transgene Protein in the CNS of the R6 and Hdex Lines

Western blot of whole brain homogenates immunostained with antibody CAG53b. Transgene protein is detected in lines R6/1, R6/2, R6/5, Hdex6, and Hdex27. The difference in the migration of the proteins reflects the size of the polyglutamine tract in each case. The sample in lane R6/5 is derived from an R6/5 homozygote and the observation of two protein bands results from the presence of different sized CAG expansions at the two R6/5 loci.

Huntingtin Immunoreactivity

Immunohistochemical analysis of htt in the control adult mouse brain showed labeling of the entire gray matter, with neuronal labeling found in all regions including the cerebral cortex, striatum, cerebellum, and spinal cord. Reaction product appeared in the cytoplasm of neuronal cell bodies and could also be detected in dendrites and axons traversing the neuropil. A similar pattern of labeling was found with three different antibodies and is consistent with previous reports of htt distribution in the primate and rodent brain using the same antisera (DiFiglia et al., 1995; Sharp et al., 1995; Bhide et al., 1996). At the ultrastructural level, reaction product was scattered throughout the cytoplasm and associated with vesicular membranes. Small patches of labeling were found in dendrites, unmyelinated axon fibers, axon terminals, and synaptic contacts. Reaction product was never found within the neuronal nucleus.

In marked contrast to the patterns of immunoreactivity seen in control animals, the most prominent feature of htt immunoreactivity in transgenic mice was the appearance of a densely stained circular inclusion within neuronal but not glial nuclei. This staining is in addition to the distribution observed in control mice. Indeed, using normal concentrations of all three antisera this inclusion was overstained, and subsequent studies used lower concentrations of antibody, producing less obvious staining of the endogenous mouse protein (compare Figures 2A and 2C). Analysis of thionin counterstained sections suggests the presence of a single htt-immunoreactive nuclear inclusion in almost all striatal neurons. An antibody that recognizes extended glutamine sequences in Western blots (Trottier et al., 1995b) recognizes the transgenic protein in these transgenic mice (Mangiarini et al., 1996), but fails to immunostain the inclusion using immunocytochemical methods. Antibodies to portions of htt not present in the transgenic protein (Gutekunst et al., 1995) fail to recognize the nuclear localization, suggesting that the endogenous mouse htt protein does not colocalize with the ectopic transgenic protein. This characteristic labeling of a single, small NII was found in all lines of transgenic mice that exhibit a neurological phenotype (6/2 and 6/1 hemizygotes, and 6/1 and 6/5 homozygotes, Figures 2E and 2F), but not in those that remain symptom free (6/0, 6/5, HDex6, HDex27, Figure 2D). We have observed many of these inclusions within neurons in the cerebral cortex, striatum, cerebellum, and the spinal cord, whereas areas such as the hippocampus, thalamus, globus pallidus, and substantia nigra contain many fewer neurons containing NII. We are currently undertaking a thorough mapping of the distribution of NII within all the trangenic lines. In semithin, toluidine blue–counterstained sections an htt-immunoreactive inclusion was seen in ~20% of neurons. At the ultrastructural level, reaction product was found to be densely accumulated within a single defined region of the nucleus that is quite distinct from the nucleolus, accessory body of Cajal (coiled body), or the sex chromatin (Barr bodies) found in female mice (Figures 3A and 3B). Occasionally, reaction product was observed traversing pores in the nuclear membrane, which we interpret to be cytoplasmic htt entering the nucleus. A dense accumulation of reaction product was also found in multivesicular bodies present in the cytoplasm of neurons that appear to be more frequent in the transgenic animals.

Nuclear Morphology

Ultrastructural analysis of the striatum in symptomatic transgenic animals reveals the presence of a prominent, solitary NII that appears as a roughly circular pale structure easily identified in toluidine blue–stained semithin sections. In thin sections, the paler dense NII is readily distinguished from the more darkly stained surrounding heterochromatin (Figure 4). There is no membrane separating the inclusion from the surrounding nuclear matrix. The structure of the NII appears to be of a fine granular nature with occasional filamentous structures. These filamentous structures are more readily apparent in the periphery around the NII. We have tried using stereoimaging (6° tilt either side of vertical at magnifications of 80,000 to 200,000) to describe more accurately the structure of the NII but cannot elucidate any additional structural detail. Clearly, if these NII do have a fibrous composition, the filaments are less than 1 to 5 nm in diameter.

We have never identified a nuclear inclusion in an astrocyte, oligodendrocyte, or microglial cell in any of the 6/2 transgenic mice, nor have we seen an NII in transgenic lines that fail to develop a phenotype (6/0, 6/5 hemizygote, Hdex27, Hdex6). Morphological investigation of the NII shows that it is larger than the nucleolus (NII average diameter, 1.65 $\pm$ 0.05 μm; nucleolus average diameter, 1.16 $\pm$ 0.03 μm) and occupies 1% of the nuclear volume (nucleolus occupies 0.33%; Figure 5). Simple calculations suggest that a single NII, 1.65 μm in diameter, present in a nucleus 7.78 μm in diameter will occur in 20% of sections 70 to 90 nm in thickness. This is consistent with the observation of an NII in one in five neurons.

In addition to the NII, striatal neurons are invariably found to have prominent and frequent indentations of the nuclear membrane and often an apparent increase in the clustering and number of nuclear pores. While nuclear indentations can be found in striatal neurons

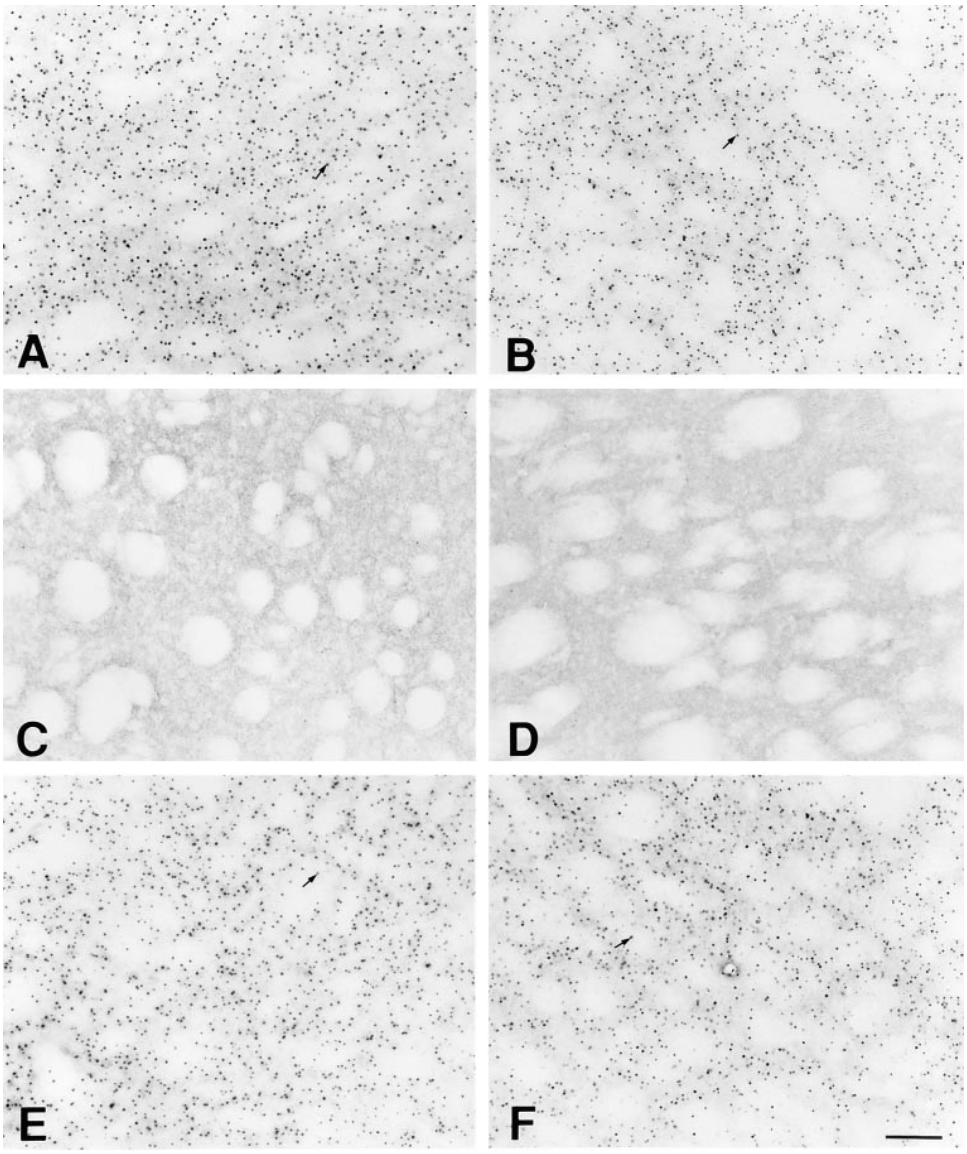

Figure 2. Huntingtin and Ubiquitin Immunoreactivity in the Striatum

Photomicrographs of htt immunoreactivity (A, C–F) or ubiquitin immunoreactivity (B) in the striatum of 6/2 (A–C), Hdex27 (D), and 6/1 (E) hemizygous mice or in 6/5 (F) homozygous mice. The section shown in (C) was incubated in antibody that had been preabsorbed with peptide and demonstrates a complete absence of nuclear staining. The htt (A, B, E, and F) and ubiquitin (B) immunoreactive nuclear inclusions are indicated by the small arrows; no such inclusions can be seen in the transgenic mouse with 18 glutamine repeats (Hdex27) (D). Pale areas in each section are the myelinated fibers of the internal capsule present throughout the darker staining striatal neuropil. Scale bar represents 100 μm for (A)–(F).

(Kemp and Powell, 1971), they are infrequent, typically occurring in 2% to 10%. However, in symptomatic transgenic mice, we find these changes in almost all the cells investigated. Both the frequency and extent of the nuclear invagination is so dramatically increased that these changes are diagnostic for the symptomatic mice. However, the increase in nuclear pore density is more subjective and requires careful quantitation. Morphometric analysis fails to detect any significant change in the size of the nucleus or the nucleolus (Figure 6), or the accessory body of Cajal (coiled body). The distribution of the heterochromatin and sex chromatin in female mice is unaltered between transgenic and control mice.

Ubiquitin Immunoreactivity

Immunocytochemical localization of ubiquitin in 6/1, 6/2, and 6/5 homozygous mice reveals a prominent single nuclear inclusion (Figure 2B), identical in appearance to that seen with antibodies to htt (compare Figures 3A and 3C with Figures 3B and 3D). Sections analyzed from control mice, HDex27, HDex6, or from 6/5 hemizygous animals reveal a low level of cytoplasmic labeling with no evidence of nuclear staining. When the ubiquitin immunoreactive nuclear inclusions are analyzed at the EM level, they are found to correspond to the nuclear inclusion seen by previous methods. While the NII appear to contain substantial amounts of ubiquitin, the multivesic-

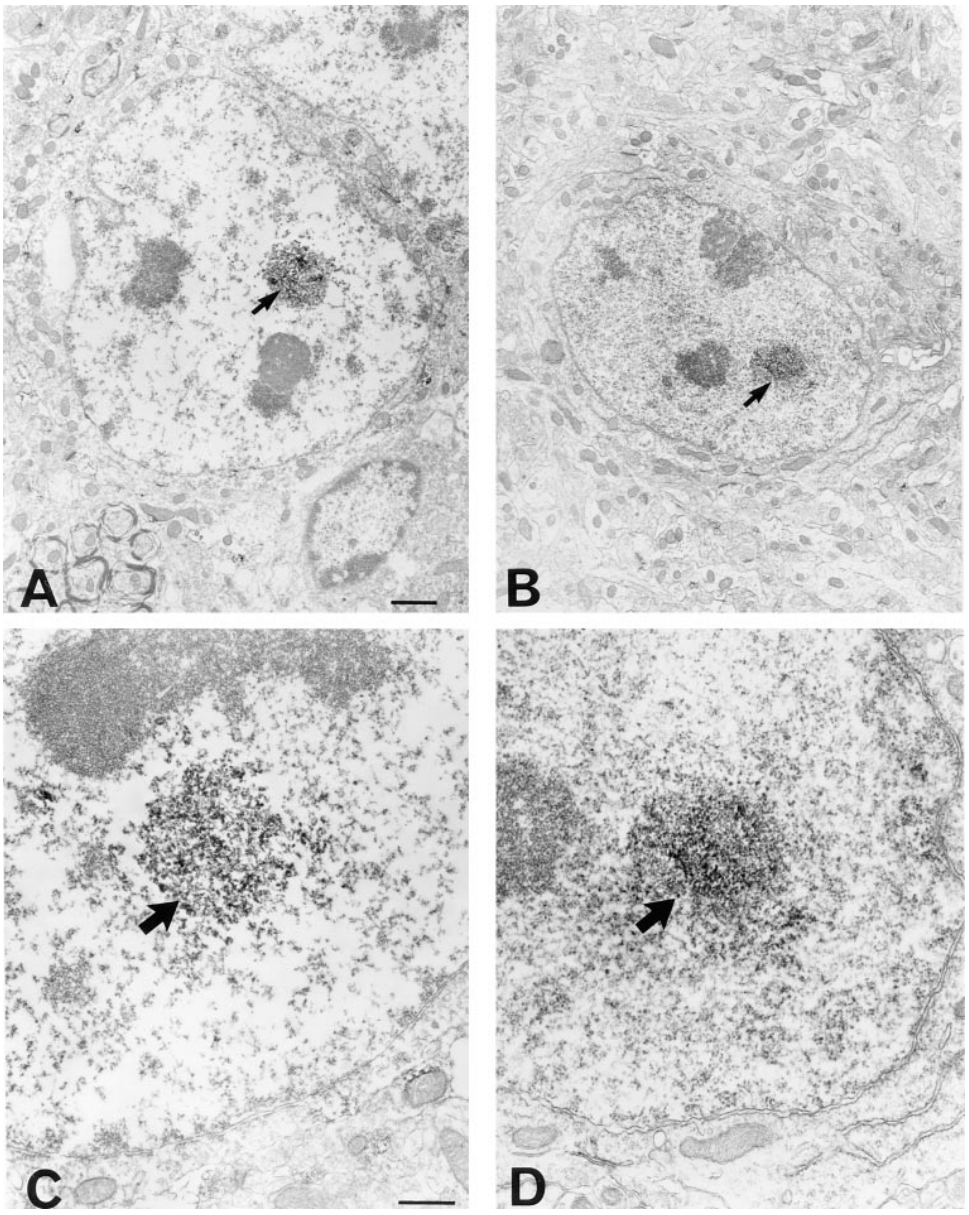

Figure 3. EM Localization of Huntingtin and Ubiquitin within the Neuronal Nucleus of Transgenic Mice

Discrete deposition of DAB reaction product within the NII with antibodies to htt (A and C) and ubiquitin (B and D). A single intensely stained inclusion is seen with both antibodies. Scale bar for (A) and (B) is 1μm and for (C) and (D) is 500 nm.

ular bodies do not, nor do we find any ubiquitin immunoreactive reaction product in structures that normally contain htt. Antibodies to tau protein or to phosphorylated epitopes of tau (Tau 134, AT8, PHF-1, ALZ 50) or to β-amyloid failed to recognize the NII. Similarly, thioflavin-S staining did not recognize a β-pleated sheet conformation for the protein deposits within the NII. Bielshowsky silver staining of neuronal nuclei readily identified the nucleolus but failed to stain NII.

Progression of Neuropathological Change

The dramatic nuclear changes we have reported thus far have all been observed in symptomatic mice of the 6/1, 6/2, or 6/5 homozygous lines. We have now analyzed the temporal sequence of the appearance for the nuclear changes we have reported in the 6/2 line (Figure 6). This is the most severely affected of the transgenic lines, with a reduction in brain weight at 5 weeks, progressive loss of body weight by 8 weeks, and onset of symptoms at around 2 months. From our initial observations, it was not clear whether the reduction in brain weight at 12 weeks was a consequence of the reduction in total body weight. This longitudinal investigation clearly demonstrates that the loss in brain weight precedes the loss in body weight (Figure 6).

The presence of htt immunoreactivity can be detected in neuronal nuclei within defined regions of the cerebral

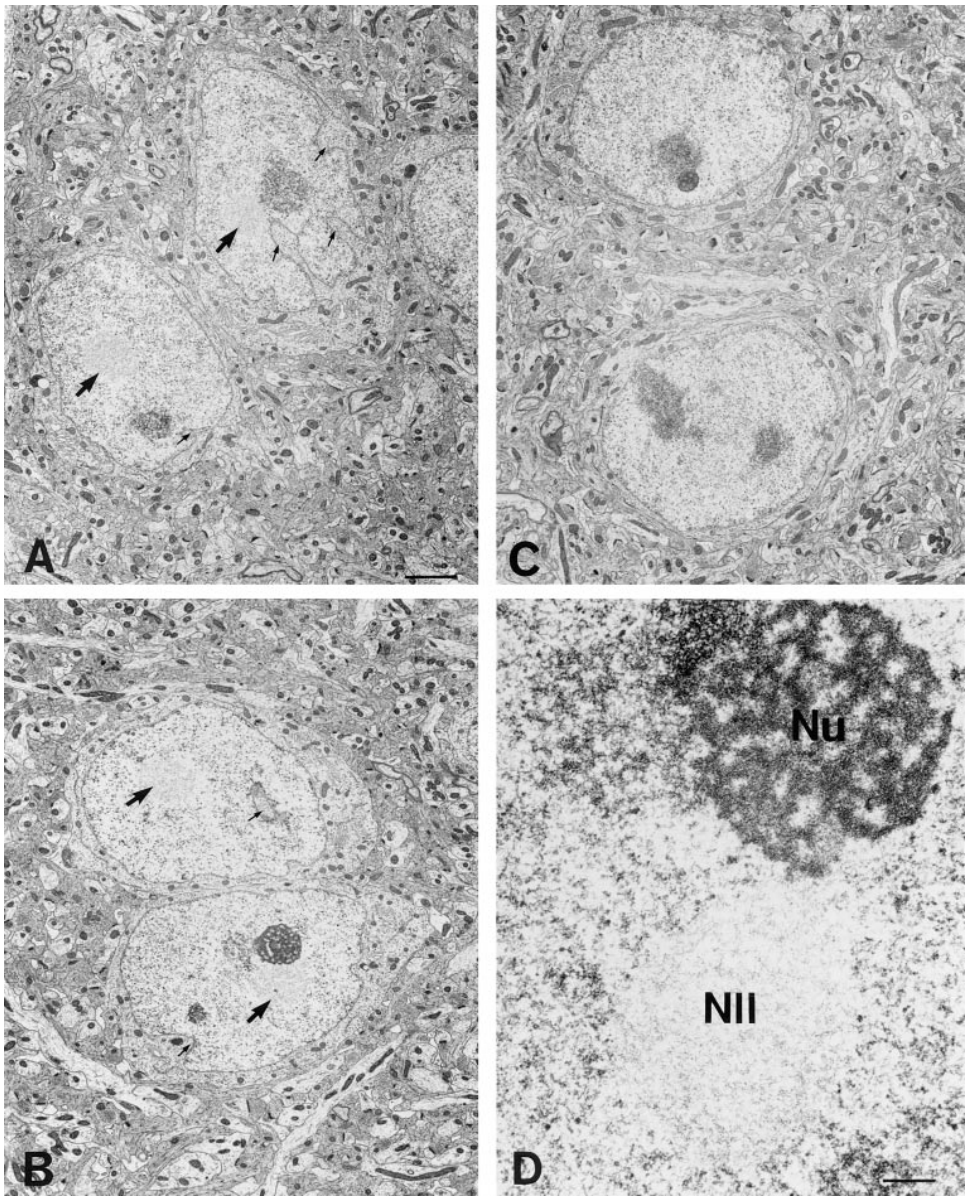

Figure 4. Ultrastructure of the Nucleus

Examples of the NII (A and B; indicated by large arrows) found within striatal neurons that have many indentations in the nuclear membrane (small arrows) demonstrated with conventional electron microscopy (osmium/uranyl/lead staining). Typically, more than 90% of neurons within the mouse striatum have a smooth nuclear profile, and all lack any inclusion (C). At higher magnifications, the NII is seen to be a pale staining structure quite distinct from the more darkly stained adjacent nucleolus (Nu) and surrounding chromatin. Scale bar for (A)–(C) is 2 μm and for (D) is 200 nm.

cortex beginning at 3.5 weeks and within the striatum at 4.5 weeks. These NII become ubiquitinated by 5 to 6 weeks and can be detected by ultrastructural analysis at 8 weeks. Morphological changes within the nuclear membrane are the latest changes to occur, first becoming apparent at 10 to 12 weeks. NII appear within the cerebral cortex before they are found in any numbers within the striatum, and they increase in size and staining density for both htt and ubiquitin immunoreactivity. The frequency and progressive increase in size of NII appears to vary dramatically between different classes of neurons. The largest inclusions can be found within the cerebral cortex, striatum, cerebellum (Purkinje cells), and the spinal cord (motor neurons). Interestingly, within the striatum inclusions are found in the vast majority of neurons but apparently not in the giant cholinergic interneurons or in the NADPH-diaphorase-containing interneurons (data not shown). We do not know if the inclusions are exclusively within projection cells within the striatum or if some interneurons contain these structures. A systematic analysis is currently being performed of the progressive appearance of NII within identified

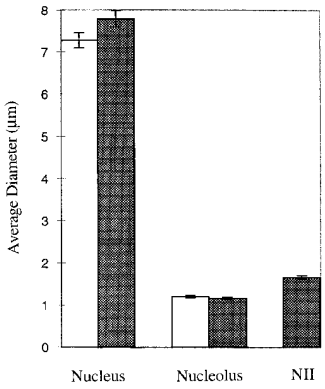

Figure 5. Morphometric Analysis of the Nucleus, Nucleolus, and NII

Histograms of the nuclear, nucleolar, and intranuclear inclusion size for striatal neurons in control (open columns) and 6/2 transgenic mice (hatched columns). There is no significant difference between the size of the nucleus or nucleolus in 13-week-old 6/2 transgenic mice and littermate controls. The NII is significantly larger than the nucleolus comprising 1% of the nuclear volume.

cell types in the CNS, PNS, and nonneuronal tissues during the development of the disease in line R6/2 and in lines with a slower progression of phenotype.

Fos B and NGFI-A Immunoreactivitity

The transcription factors Fos B and NGFI-A are constitutively expressed in neurons throughout the mouse CNS, and in immunocytochemical preparations neuronal nuclei are characteristically densely labeled with a prominent sparing of the nucleolus. Ultrastructural analysis of neuronal nuclei immunostained for either Fos B or NGFI-A in transgenic mice reveals a dense accumulation of reaction product throughout the nuclear matrix, with a notable exclusion over the nucleolus and the NII (Figure 7). In all transgenic lines that fail to develop symptoms, the nucleus is uniformly stained with the single exception of the nucleolus.

Discussion

We have identified a novel molecular mechanism responsible for the progressive neurological dysfunction occurring in mice that are transgenic for the HD mutation. Neurons within the striatum of these mice contain an NII that is apparent upon ultrastructural analysis and contains the proteins htt and ubiquitin. This firmly establishes a role for the expressed protein in the mechanism of mutation-induced disease. The NII occurs in all transgenic lines that progress to exhibit symptoms (6/2, 6/1 hemizygotes and 6/1, 6/5 homozygotes) but not in asymptomatic lines (6/0, 6/5 hemizygotes, HDex6, and HDex27), strongly implicating a causative role for the NII in the generation of neurological dysfunction. The appearance of an NII is followed by a pronounced indentation of the nuclear membrane and an apparent increase in the density of nuclear pores. This increase is not confined to regions of indentation but appears throughout the nuclear membrane.

Remarkably, all three of these ultrastructural nuclear changes have previously been reported in EM studies from human HD patients. The most prominent ultrastructural change reported in biopsies of the cerebral cortex and caudate nucleus of 18 patients with HD (Roizin et al., 1979) is the presence of a nuclear inclusion strikingly similar to those presented in this study. Other studies report the marked change in neuronal membranes, namely the increase in nuclear indentation (Roos and Bots, 1983; Bots and Bruyn, 1987) and increase in density of nuclear pores (Tellez-Nagel et al., 1974). It is noteworthy that these changes were predominantly found in biopsy material, since ultrastructural studies of postmortem brain from patients with HD have rarely detected similar changes (Forno and Norville, 1979). Probably because of the great dilution of the nucleoprotein, the neuronal nucleus is more difficult to preserve for fine structural studies than are most other nuclei (Peters et al., 1991). More recently, immunocytochemistry using Ab 1 has detected an intranuclear accumulation of htt in the cortex and striatum of postmortem HD brains (M. D., unpublished data).

The appearance of htt and ubiquitin within the neuronal nucleus precedes any phenotypic change in the mice but is invariably linked to the subsequent development of neurological symptoms. The associated nuclear changes are likely to occur in response to this cellular dysfunction. Throughout the symptomatic period, the nucleus, nucleolus, accessory body of Cajal (coiled bodies), and sex chromatin (Barr bodies) do not change in size or distribution between transgenic mice and littermate controls. The NII are not associated with the coiled bodies and are singular, larger structures than the more frequent (2 to 6 per cell) and smaller (0.1 to 1.0 μm) structures termed gems (Liu and Dreyfuss, 1996). We therefore are confident that the NII identified in this study are not those termed gems and implicated in neurodegeneration in spinal muscular atrophy (Liu and Dreyfuss, 1996). An increase in nuclear membrane indentation and the relative density of nuclear pores is a feature of the neuronal response to axonal injury (Lieberman, 1971) and is thought to reflect an increase in communication between the cytoplasmic and nuclear compartments of the perikaryon prior to axonal regeneration. Successful regeneration is however invariably accompanied by an increase in nucleolar size, indicating increased protein synthesis, probably the most sensitive indicator of the functional state of a neuronal cell (Lieberman, 1971). It seems that striatal neurons containing an NII are attempting the first stages of an ultimately unsuccessful regenerative response, a situation somewhat reminiscent of the simultaneous dendritic regeneration and degeneration found in Golgi impregnation of neurons from postmortem human HD striatum (Graveland et al., 1985).

In control and presymptomatic mice, the transgene protein appears to have a subcellular localization consistent with the endogenous htt. Its translocation to the nucleus occurs just prior to the onset of symptomatology and most probably represents the dominant gain of function. The molecular events that trigger the translocation to the nucleus are not clear. The transgene protein does not itself contain a nuclear localization signal and

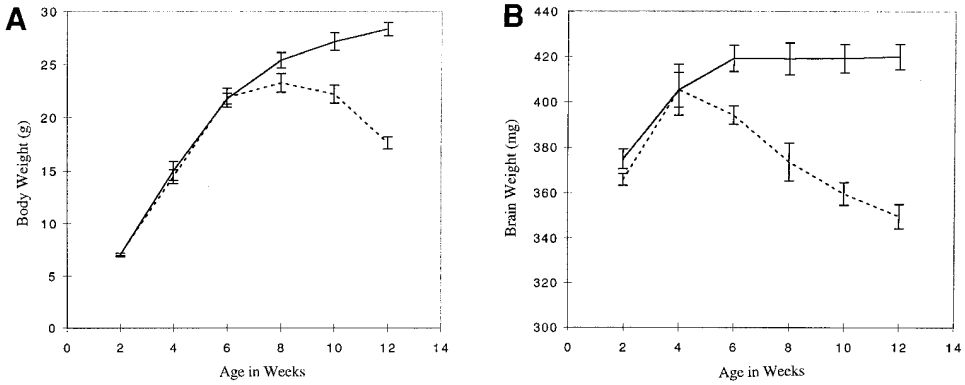

C

Disease Progression in 6/2 HT Mice

PHENOTYPE														
Brain Weight Loss	-	-	-	-	-	+	++	++	+++	+++	+++	+++	+++	+++
Body Weight Loss	-	-	-	-	-	-	-	+	+	+	++	+++	+++	+++
Symptoms	-	-	-	-	-	-	-	-	-	+	+	++	++	+++
NEUROPATHOLOGY														
htt in Nucleus	-	-	-	-	+	+	+	++	++	+++	+++	+++	+++	+++
Ubiquitin in Nucleus	-	-	-	-	-	-	+	+	+	+	++	+++	+++	+++
NII by EM	-	-	-	-	-	-	-	+/-	+	+	++	++	++	++
Nuclear Indentation	-	-	-	-	-	-	-	-	-	+	+	+	++	++
Age in Weeks	**2**	**3**	**3.5**	**4**	**4.5**	**5**	**6**	**7**	**8**	**9**	**10**	**11**	**12**	**13**

Figure 6. Progression of Pathology and Phenotype in the 6/2 Line

Timing and progression of the reduction in body weight (A) and brain weight (B) in a series of R6/2 transgenes and littermate controls. (C) Correlation of the changes in body and brain weight with the progression of the neurological and neuropathological phenotype of 6/2 transgenic mice.

therefore may cross the nuclear membrane by complexing with one or more cellular proteins. A number of proteins that interact with htt have thus far been identified and include HAP1 (Li et al., 1995), HIP1 (Wanker et al., 1997), ubiquitin-conjugating enzyme (Kalchman et al., 1996), and GAPDH (Burke et al., 1996). Immunocytochemical colocalization of htt-interacting proteins within NII in the brains of symptomatic mice will be informative as to their possible involvement in the pathogenesis of HD. It has been suggested that polygln repeats may form polar zippers, allowing them to interact with other proteins or to homodimerize (Perutz, 1996). The observation that recombinant protein generated from exon 1 of the *HD* gene carrying $(CAG)_{53}$ can form aggregates in vitro may support a homodimerization model for the mutant protein (Scherzinger et al., 1997). Antibodies to sequences present within mouse htt but not the transgene do not recognize the NII, arguing against any potential interaction between the transgene and the endogenous mouse htt. htt has been shown to be specifically cleaved by apopain, a cysteine protease with a key role in the proteolytic events leading to apoptosis (Goldberg et al., 1996). It has been suggested that apopain cleavage results in an N-terminal fragment containing the polygln expansion and that this truncated protein is toxic to certain cells. A mechanism of this type is supported by preliminary observations indicating that it is only the N terminus of htt that is present in the nucleus of postmortem brains (M. D., unpublished data). Further evidence is provided by the observation that the C terminus of the ataxin-3 protein, containing a polygln repeat expansion, is more toxic to COS cells in transient transfection assays that the entire ataxin-3 protein carrying an identical expansion (Ikeda et al., 1996). It is possible that the truncated version of htt present in the R6 lines represents the toxic product; however, the delay in the accumulation of the protein in the nucleus and the onset of symptoms still indicate the necessity of a threshold step.

The polygln-containing proteins that have been found to be mutated in the neurodegenerative diseases identified thus far are all widely expressed, and the factors that convey the specific patterns of neurodegeneration are not understood. It may have been expected that as the R6 transgene protein contains only the N-terminal 3% of htt, the transgenes would represent a generic CAG mouse rather than a specific model of HD. The observed phenotype does not support this, as it displays many features of early onset HD and does not include an overt cerebellar ataxia as described for the SCA mouse models (Burright et al., 1995; Ikeda et al., 1996). We have shown here that the appearance of an NII containing first htt and then ubiquitin immunoreactivity within certain regions of cerebral cortex followed by the striatum is consistent with the earliest neuropathological studies that identified these as the principal sites of degeneration in postmortem HD brain (Alzheimer, 1911). The pronounced indentation of the nuclear membrane accompanied by an increased clumping of heterochromatin is suggestive of the earliest stage of apoptotic change; however, we never detect apoptotic nuclei in either the

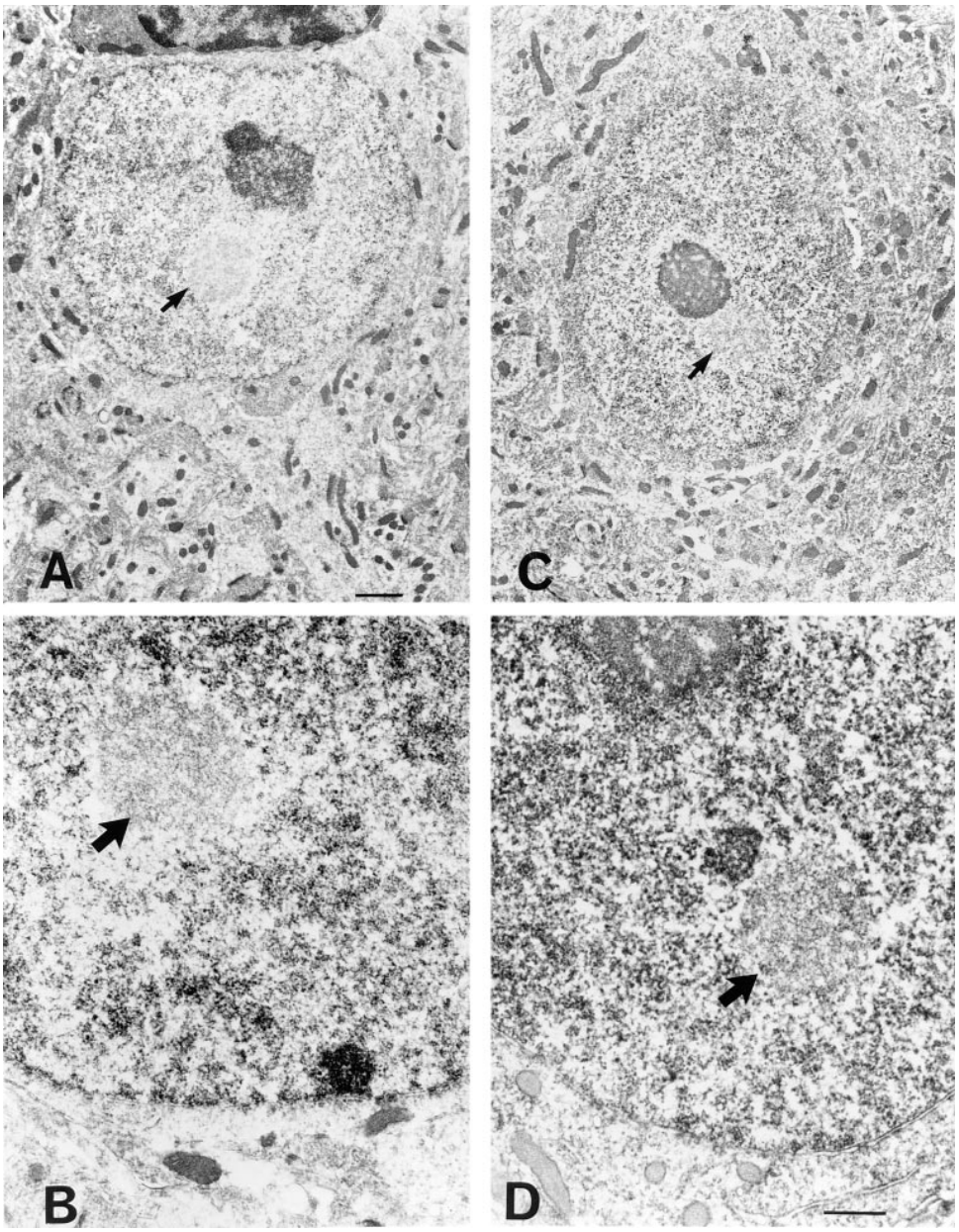

Figure 7. Exclusion of NGFI-A and Fos B Immunoreactivity from NII

Ultrastructural localization of the transcription factors NGFI-A (A and B) and Fos B (C and D) within the nucleus: reaction product is present throughout the nucleoplasm but is not found overlying the nucleolus or the NII. Scale bar for (A) and (C) is 1 μm and for (B) and (D) is 500 nm.

striatum or the neocortex. It appears that these early morphological changes do not proceed to neuronal cell death in the R6/2 line. The localization of NII within the majority of striatal neurons but not the cholinergic or NADPH-diaphorase-containing interneurons parallels the patterns of cell death observed in HD. The neurodegenerative process of HD appears preferentially to affect the GABA-containing projection cells prior to the involvement of striatal interneurons (Kowall et al., 1987). The cellular localization of NII in the R6/2 transgenes therefore closely parallels the pattern of neurodegeneration seen in the striatum in HD, suggesting that the transgene is sufficient to convey at least in part an HD-specific pattern of cellular dysfunction. The R6 transgene is under the control of endogenous promoter elements and therefore may be expected to be expressed at cellular levels comparable to endogenous htt. Quantitative analysis of striatal cellular htt expression levels in the rat (Kosinski et al., 1997) also shows an expression pattern consistent with the NII localization, implying that the rate of formation of the NII may be largely dependent upon expression levels. This model is supported by the observation that the NIIs appear earlier in homozygote lines as compared to their hemizygous counterparts, and that these mice have a correspondingly earlier age of onset and rapid progression

of the phenotype. Therefore, it follows that a reduction in the level of the mutant protein may provide an avenue for therapeutic intervention.

The NII appears remarkably homogeneous throughout its structure with the possible exception of isolated fibers at the periphery. This is mirrored by an even distribution of the two proteins in the NII. This is in contrast to a recently described inclusion found predominantly within the cytoplasm of glia in a transgenic mouse model of amyotrophic lateral sclerosis (Bruijn et al., 1997), which has a dense central core with a lighter staining peripheral halo. The expanded polygln tract must confer a conformational change or allow molecular interactions that present a target for ubiquitination but do not result in protein degradation. Western blot analysis of the transgene protein has not consistently shown the presence of higher molecular weight products, suggesting that the protein within these structures is either disrupted upon extraction or, more probably, is insoluble in the extraction buffer. Interestingly, a high molecular weight product was shown to be present in the pellet of cell lysates prepared from COS cells transiently transfected with the C terminus of ataxin-3 carrying $(CAG)_{79}$ (Ikeda et al., 1996). This band appeared as a smear, which would be consistent with ubiquitination. Only a single NII is detected in each cell, and it is never associated with the nuclear membrane but can occur adjacent to the nucleolus. The mechanism whereby the presence of an NII brings about cellular dysfunction resulting in neurological symptoms is not clear. The pale staining characteristics of the NII at the ultrastructural level are a result of the htt/ubiquitin protein precluding the binding of transcription factors to DNA (Fos B and NGFI-A) or even heavy metals to DNA (EM studies). This might suggest that the protein aggregate may either displace DNA from the nuclear matrix, or it may be so tightly bound to the chromatin that a protein–DNA complex, if formed, will not be solubilized by conventional treatments in biochemical investigations. Irrespective of the molecular mechanism of action of the NII, its presence brings about major structural changes in the nucleus, namely indentation of the nuclear membrane and an increase in the nuclear pore density. It is strikingly apparent that the presence of the NII can bring about pronounced neurological dysfunction in the absence of obvious cell death. These results clearly highlight the neuronal nucleus as the primary site for cellular dysfunction and suggest that changes in other organelles (e.g., mitochondria, which appear with a normal morphology and in similar numbers to control mice) are secondary.

Our demonstration of a novel gain of function, acquired by expansion of the polygln sequence within htt, may prove to be a common mechanism for all neurodegenerative diseases due to polygln repeat expansion. For in addition to the nuclear localization of htt in HD brain (M. D., unpublished data), a nuclear localization of the ataxin-3 protein has been identified in several regions of the brain from a Machado-Joseph disease patient (Paulson et al., 1997). Further analysis of neurons from both postmortem human brain and from transgenic animal models will rapidly confirm this.

Experimental Procedures

Transgenic Mice

Four lines of transgenic mice derived from a chimeric founder together with their nontransgenic littermate controls were studied (see Mangiarini et al., 1996, for a full description of genotype/phenotype of the transgenic lines used in this study). These comprised: 31 6/2 mice and 30 controls, ranging in age from 15 days to 13 weeks and 3 days; three 6/5 hemizygous (12 to 14 months) and three littermate controls; five 6/5 homozygous (13 to 14 months) and three littermate controls; eight 6/1 hemizygotes (5 to 9 months) and two littermate controls; one 6/1 homozygote (5 months); and one 6/0 hemizygote (7.5 months). Ages of neurological symptoms within these lines were approximately: 6/2 hemizygotes, 2 months; 6/1 homozygotes, 3 months; 6/1 hemizygotes, 5 months; and 6/5 homozygotes, 9 months. Additionally, two lines expressing the identical construct carrying a $(CAG)_{18}$ tract were analyzed. These were one Hdex6 (7 months) and one Hdex27 mouse (4 months). Approximately seven male R6/2 transgenes and seven littermate controls were weighed, deeply anesthetized, and perfused at 2-week intervals from 2 to 12 weeks to allow a longitudinal study of the progression of the disorder. Brains were removed and weighed postfixation. DNA was prepared from tail biopsy and genotyping was as previously described (Mangiarini et al., 1996).

Tissue Processing for Light Microscopy

Animals were anesthetized with an overdose of sodium pentobarbitone (Sagatal, 100 mg/kg, intraperitoneally) and perfused through the left cardiac ventricle with 35 to 50 ml of a 2% paraformaldehyde/lysine/periodate fixative in phosphate buffer (pH 7.4). Brains were carefully removed and placed into fixative for 4 to 6 hr before being transferred to 30% sucrose in 0.1 M Tris (pH 7.4) for 48 hr at 4°C. Brains were mounted in Tissue-Tek OCT compound (Miles Laboratories), frozen with powdered solid CO_2, and sectioned in the coronal plane at 40 μm on a sledge microtome. Sections were mounted onto gelatinized glass slides and allowed to dry overnight. Alternate sections were stained for Nissl substance with thionin before all sections were rapidly dehydrated through ethanols, cleared in Histoclear (National Diagnostics), and coverslipped.

Tissue Processing for Electron Microscopy

Animals were anesthetized as described above and then perfused through the left cardiac ventricle with 35 to 50 ml of 4% paraformaldehyde and either 0.5% glutaraldehyde or 0.1% glutaraldehyde in 0.1 M Millonigs phosphate buffer (pH 7.4). The brain was removed from the skull and placed in fresh fixative overnight at 4°C. Coronal sections (50 to 200 μm) were cut on an Oxford Vibratome (Lancer) and collected in serial order in 0.1 M phosphate buffer. After being osmicated (30 min in 1% OsO_4 in 0.1 M phosphate buffer), the sections were stained for 15 min in 0.1% uranyl acetate in sodium acetate buffer at 4°C, dehydrated in ethanols, cleared in propylene oxide, and embedded in Araldite between two sheets of Melanex (ICI). Semithin (1 μm) sections were cut with glass knives and stained with toluidine blue adjacent to thin sections cut with a diamond knife on a Reichert Ultracut ultramicrotome. The sections were collected on mesh grids coated with a thin formavar film, counterstained with lead citrate, and viewed in a Jeol 1010 electron microscope.

Immunocytochemistry

Sections were incubated free-floating in primary antibodies at 4°C for 72 hr prior to processing with biotinylated secondary antibody (2 hr) and ABC complex (2 hr, Vector Elite). All washes were in 0.1 M Tris (pH 7.4) for light microscopy and 0.1 M sodium phosphate buffer for EM. Sites of peroxidase enzyme activity were visualized by incubating sections in diaminobenzidine (25 mg/100 ml) and H_2O_2 (0.003%). Sections were then processed for EM or light microscopy as detailed above. The antibodies used in this study that recognize both exon 1 of the human and mouse htt protein were Ab 1 (1:600; DiFiglia et al., 1995), AB 78 (1:1000; Sharp et al., 1995), HD1, and CAG 53b (1:2000; E. E. W. and H. Lehrach, unpublished data). Ab 1 and Ab 78 were raised to synthetic peptides corresponding to the

first 17 amino acids of htt, while CAG 53b and HD1 were raised to fusion proteins. All three antisera recognized the NII in sections prepared for both light and electron microscopy. The NII was unstained in sections that were either incubated in Ab 1 preabsorbed with peptide antigen (50 μg) or in which the primary antibody was omitted. The antibody to ubiquitin (Dako) was used at 1:1000 and has been extensively characterized (Lowe et al., 1989). Antibodies to Fos B (1:5000; Ebling et al., 1996) and NGFI-A (ZIF 268, 1:2000; Wisden et al., 1990) detect constitutive nuclear staining in both the rat and mouse that is abolished by prior absorption with the peptide antigen. The Fos B antibody is raised against a synthetic peptide corresponding to the N-terminal sequence of Fos B and therefore recognizes both Fos B and ΔFos B (Hollen et al., 1997). Antibodies to tau (Tau 134, Alz 50, PHF-1, and AT8) and β-amyloid have previously been described (Spillantini et al., 1990; Goedert et al., 1992).

Protein Analysis

Frozen brain was homogenized in 1 ml of 62.5 mM Tris (pH 6.8), 2% SDS, 5% 2-mercaptoethanol, 10% glycerol, and 0.001% bromophenol blue. Homogenates were diluted 1:1 with water, boiled for 10 min, spun for 25 min at high speed at 4°C, and the supernatant was transferred to a fresh tube. Twenty microliters of supernatant (50 μg) was loaded onto a 10% SDS-PAGE gel. Kaleidoscope prestained standards were used as size markers (Bio-Rad). Proteins were transferred to PVDF membranes (Bio-Rad) that were blocked at 4°C overnight in PBS with 5% nonfat dry milk. Immunoprobing with polyclonal antibody CAG53b was at 1:2000 dilution in PBS with 0.5% nonfat dry milk for 2 hr at room temperature. Washes were in PBS. Detection was by use of the ECL kit (Amersham).

Acknowledgments

We thank Amarbirpal Mahal for genotype analysis, Michel Goedert for generous gifts of antibodies to tau and β-amyloid, Gerrard Evan and David Hancock for antibodies to NGFI-A, Fran Ebling for antibodies to Fos B, Steven Hersch for antibodies to htt (HD3.10.6), John Parnavelas for expert advice on electron microscopy, and Adrienne Knight for proof reading the manuscript. This work was supported by the Medical Research Council, the Wellcome Trust (M/96/262), the Hereditary Disease Foundation (in the form of an award donated by Harry Liebermann), the Special Trustees of Guy's and St. Thomas' Hospitals, the European Union, and the Deutsche Forschungsgemeinschaft.

Received May 7, 1997; revised June 19, 1997.

References

Alzheimer, A. (1911). Über die anatomische Grundlage der Huntingtonschen chorea und der choreatischen Bewegungen überhaupt. Z. Ges. Neurol. Psychiat. *3*, 566–567.

Aronin, N., Chase, K., Young, C., Sapp, E., Schwarz, C., Matta, N., Kornreich, R., Landwehrmeyer, B., Bird, E., Beal, M.F., et al. (1995). CAG expansion affects the expression of mutant huntingtin in the Huntington's disease brain. Neuron *15*, 1193–1201.

Bates, G.P., Mangiarini, L., Mahal, A., and Davies, S.W. (1997). Transgenic models of Huntingtons disease. Hum. Mol. Genet., in press.

Bhide, P., Day, M., Sapp, E., Schwarz, C., Sheth, A., Kim, J., Young, A.B., Penney, J., Golden, J., Aronin, N., and DiFiglia, M. (1996). Expression of normal and mutant huntingtin in the developing brain. J. Neurosci. *16*, 5523–5535.

Bots, G.Th.A.M., and Bruyn G.W. (1987). Neuropathological changes of the nucleus accumbens in Huntingtons chorea. Acta Neuropathol. *55*, 21–22.

Bruijn, L.I., Becher, M.W., Lee, M.K., Anderson, K.L., Jenkins, N.A., Copeland, N.G., Sisodia, S.S., Rothstein, J.D., Borchelt, D.R., Price, D.L., and Cleveland, D.W. (1997). ALS-linked SOD1 mutant G85R mediates damage to astrocytes and promotes rapidly progressive disease with SOD1-containing inclusions. Neuron *18*, 327–338.

Burke, J.R., Enghild, J.J., Martin, M.E., Jou, Y.-S., Myers, R.M., Roses, A.D., Vance, J.M., and Strittmatter, W.J. (1996). Huntingtin and DRPLA proteins selectively interact with the enzyme GAPDH. Nature Med. *2*, 347–350.

Burright, E.N., Clark, H.B., Servadio, A., Matilla, T., Fedderson, R.M., Yunis, W.S., Duvick, L.A., Zoghbi, H.Y., and Orr, H.T. (1995). SCA1 transgenic mice: a model for neurodegeneration caused by an expanded CAG trinucleotide repeat. Cell *82*, 937–948.

de la Monte, S.M., Vonsattel, J.-P., and Richardson, E.P. (1988). Morphometric demonstration of atrophic changes in the cerebral cortex, white matter and neostriatum in Huntington's disease. J. Neuropathol. Exp. Neurol. *47*, 516–525.

De Rooij, K.E., Dorsman, J.C. Smoor, M.A., Den Dunnen, J.T. and Van Ommen, G.-J.B. (1996). Subcellular localization of the Huntingtons disease gene product in cell lines by immunofluorescence and biochemical subcellular fractionation. Hum. Mol. Genet. *5*, 1093–1099.

DiFiglia, M., Sapp, E., Chase, K., Schwarcz, C., Meloni, A., Young, C., Martin, E., Vonsattel, J.-P., Carraway, R., Reeves, S.A., Boyce, F.M., et al. (1995). Huntingtin is a cytoplasmic protein associated with vesicles in human and rat brain neurons. Neuron *14*, 1075–1081.

Duyao, M.P., Auerbach, A.A., Ryan, A., Persichetti, F., Barnes, G.T., McNeil, S.M., Ge, P., Vonstattel, J.-P., Gusella, J.F., Joyner, A.L., and MacDonald, M.E. (1995). Inactivation of the mouse Huntington's disease gene homolog *Hdh*. Science *269*, 407–410.

Ebling, F.J.P., Maywood, E.S., Mehta, M., Hancock, D.C., Mc Nulty, S., De Bono, J., Bray, S.J., and Hastings, M.H. (1996). Fos B in the surrachiasmatic nucleus of the Syrian and Siberian hamster. Brain Res. Bull. *41*, 257–268.

Forno, L.S., and Norville R.L. (1979). Ultrastructure of the neostriatum in Huntingtons and Parkinsons disease. In Advances in Neurology 23, Huntingtons Disease, T.N. Chase, N.S. Wexler, and A. Barbeau, eds. (New York: Raven Press), pp. 95–122.

Goedert, M., Spillantini, M.G., Cairns, N.J., and Crowther, R.A. (1992). Tau proteins of Alzheimer paired helical filaments: abnormal phosphorylation of all six brain isoforms. Neuron *8*, 159–168.

Goldberg, Y.P., Nicholson, D.W., Rasper, D.M., Kalchman, M.A., Koide, H.B., Graham, R.K., Bromm, M., Kazemi-Esfarjani, P., Thornberry, N.A., Vaillancourt, J.P., and Hayden, M.R. (1996). Cleavage of huntingtin by apopain, a proapoptotic cysteine protease, is modulated by the polyglutamine tract. Nature Genet. *13*, 442–449.

Graveland, G.A., Williams, R.S., and DiFiglia, M. (1985). Evidence for degenerative and regenerative changes in neostriatal spiny neurons in Huntingtons disease. Science *227*, 770–773.

Gutekunst, C.A., Levey, A.I., Heilman, D.J., Whaley, W.L., Yi, H., Nash, N.R., Rees, H.D., Madden, J.J., and Hersch, S.M. (1995). Identification and localization of huntingtin in brain and human lymphoblastoid cell lines with anti-fusionprotein antibodies. Proc. Nat. Acad. Sci. USA *92*, 8710–8714.

Harper, P.S. (1991). Huntingtons Disease, Major Problems in Neurology *22* (London: W.B. Saunders).

Hedreen, J.C., and Folstein, S.E. (1995). Early loss of neostriatal neurons in Huntingtons disease. J. Neuropathol. Exp. Neurol. *54*, 105–120.

Hollen, K.M., Nakabeppu, Y., and Davies, S.W. (1997). Changes in the expression of ΔFos B and the Fos family proteins following NMDA receptor activation in the rat srtiatum. Mol. Brain Res. *47*, 31–43.

Huntingtons Disease Collaborative Research Group. (1993). A novel gene containing a trinucleotide repeat that is unstable on Huntingtons disease chromosomes. Cell *72*, 971–983.

Ide, K., Nukina, N., Masuda, N., Goto, J., and Kanazawa, I. (1995). Abnormal gene product identified in Huntington's disease lymphocytes and brain. Biochem. Biophys. Res. Comm. *209*, 1119–1125.

Ikeda, H., Yamaguchi, M., Sugai, S., Aze, Y., Narumiya, S., and Kakizuka, A. (1996). Expanded polyglutamine in the Machado-Joseph disease protein induces cell death in vitro and in vivo. Nature Genet. *13*, 196–202.

Jou, Y.-S., and Myers, R.M. (1995). Evidence from antibody studies that the CAG repeat in the Huntington disease gene is expressed in the protein. Hum. Mol. Genet. *4*, 465–469.

Kalchman, M.A., Graham, R.K., Xia, G., Koide, H.B., Hodgson, J.G., Graham, K.C., Goldberg, Y.P., Gietz, R.D., Pickart, C.M., and Hayden, M.R. (1996). Huntingtin is ubiquitinated and interacts with a specific ubiquitin-conjugating enzyme. J. Biol. Chem. *32*, 19385–19394.

Kemp, J.M., and Powell, T.P.S. (1971). The structure of the caudate nucleus of the cat: light and electron microscopy. Philos. Trans. R. Soc. Lond. [Biol] *262*, 383–401.

Kosinski, C.M., Cha, J.-H., Young, A.B., Persichetti, F., MacDonald, M., Gusella, J.F., Penney, J.B., and Standaert, D.G. (1997). Huntingtin immunoreactivity in the rat neostriatum: differential accumulation in projection and interneurones. Exp. Neurol., in press.

Kowall, N.W., Ferrante, R.J., and Martin, J.B. (1987). Patterns of cell loss in Huntingtons disease. Trends Neurosci. *10*, 24–29.

Li, X.-J., Li, S.-H., Sharp, A.H., Nucifora, F.C., Schilling, G., Lanahan, A., Worley, P., Snyder, S.H., and Ross, C.A. (1995). A huntingtin-associated protein enriched in brain with implications for pathology. Nature *378*, 398–402.

Lieberman, A.R. (1971). A review of the principal features of perikaryal responses to axon injury. Int. Rev. Neurobiol. *14*, 49–124.

Liu, Q., and Dreyfuss, G. (1996). A novel nuclear structure containing the survival of motor neurons protein. EMBO J. *15*, 3555–3565.

Lowe, J., Aldridge, F., Lennox, G., Doherty, F., Jefferson, D., Landon M., et al. (1989). Inclusion bodies in motor cortex and brainstem of patients with motor neurone disease are detected by immunocytochemical localization of ubiquitin. Neurosci. Lett. *105*, 7–13.

Mangiarini, L., Sathasivam, K., Seller, M., Cozens, B., Harper, A., Hetherington, C., Lawton, M., Trottier, Y., Lehrach, H., Davies, S.W., and Bates, G.P. (1996). Exon 1 of the HD gene with an expanded CAG repeat is sufficient to cause a progressive neurological phenotype in transgenic mice. Cell *87*, 493–506.

Mangiarini, L., Sathasivam, K., Mahal, A., Mott, R., Seller, M. and Bates, G.P. (1997). Instability of highly expanded CAG repeats in mice transgenic for the Huntingtons disease mutation. Nature Genet. *15*, 197–200.

Myers, R.H., Vonsattel, J.P., Stevens, T.J., Cupples, L.A., Richardson, E.P., Martin, J.B., and Bird, E.D. (1988). Clinical and neuropathological assessment of severity in Huntington's disease. Neurology *38*, 341–347.

Myers, R.H., Vonsattel, J.P., Paskevich, P.A., Kiely, D.K., Stevens, T.J., Cupples, L.A., Richardson, E.P., and Bird, E.D. (1991). Decreased neuronal and increased oligodendroglial densities in Huntington's disease caudate nucleus. J. Neuropathol. Exp. Neurol. *50*, 729–742.

Nasir, J., Floresco, S.B., O'Kusky, J.R., Diewert, V.M., Richman, J.M., Zeisler, J., Borowski, A., Marth, J.D., Phillips, A.G., and Hayden, M.R. (1995). Targeted disruption of the Huntington's disease gene results in embryonic lethality and behavioral and morphological changes in heterozygotes. Cell *81*, 811–823.

Paulson, H.L., Das, S.S., Crino, P.B., Perez, M.K., Patel, S.C., Gotsdiner, D., Fischbeck, K.H., and Pittman, R.N. (1997). Machado-Joseph disease gene product is a cytoplasmic protein widely expressed in brain. Ann. Neurol. *41*, 453–462.

Perutz, M.F. (1996). Glutamine repeats and inherited neurodegenerative diseases: molecular aspects. Curr. Opin. Struct. Biol. *6*, 848–858.

Peters, A., Palay, S.L., and Webster, H.deF. (1991). The Fine Structure of the Nervous System. (New York: Oxford University Press).

Roizin, L., Stellar, S., and Liu, J.C. (1979). Neuronal nuclear-cytoplasmic changes in Huntingtons chorea: electron microscope investigations. In Advances in Neurology 23, Huntingtons Disease, T.N. Chase, N.S. Wexler, and A. Barbeau, eds. (New York: Raven Press), pp. 95–122.

Roos, R.A.C., and Bots, G.Th.A.M. (1983). Nuclear membrane indentations in Huntingtons chorea. J. Neurol. Sci. *61*, 37–47.

Ross, C.A. (1995). When more is less: pathogenesis of glutamine repeat neurodegenerative diseases. Neuron *15*, 493–496.

Scherzinger, E., Lurz, R., Turmaine, M., Mangiarini, L., Hollenbach, B., Hasenbank, R., Bates, G.P., Davies, S.W., and Wanker, E.E. (1997). Huntingtin-encoded polyglutamine expansions form amyloid-like protein aggregates in vitro and in vivo. Cell, this issue, *90*, 549–558.

Schilling, G., Sharp, A.H., Loev, S.J., Wagster, M.V., Li, S.-H., Stine, O.C., and Ross, C.A. (1995). Expression of the Huntington's disease (IT15) protein product in HD patients. Hum. Mol. Genet. *4*, 1365–1371.

Sharp, A.H., Loev, S.J., Schilling, G., Li, S.-H., Li X.-J., Bao, J., Wagster, M.V., Kotzuk, J.A., Steiner, J.P., Lo, A., et al. (1995). Widespread expression of Huntington's disease gene (IT15) protein product. Neuron *14*, 1065–1074.

Spillantini, M.G., Goedert, M., Jakes, R., and Klug, A. (1990). Topographical relationship between beta-amyloid and tau protein epitopes in tangle-bearing cells in Alzheimer disease. Proc. Natl. Acad. Sci. USA *87*, 3952–3956.

Tellez-Nagel, I., Johnson B., and Terry, R.D. (1974). Studies on brain biopsies of patients with Huntingtons chorea. J. Neurocytol. *3*, 308–332.

Trottier, Y., Devys, D., Imbert, G., Sandou, F., An, I., Lutz, Y., Weber, C., Agid, Y., Hirsch, E.C., and Mandel, J.-L. (1995a). Cellular localization of the Huntington's disease protein and discrimination of the normal and mutated forms. Nature Genet. *10*, 104–110.

Trottier, Y., Lutz, Y., Stevanin, G., Imbert, G., Devys, D., Cancel, G., Sandou, F., Weber, C., David, G., Tora, L., et al. (1995b). Polyglutamine expansion as a pathological epitope in Huntingtons disease and four dominant cerebellar ataxias. Nature *378*, 403–406.

Vonsattel, J.-P., Myers, R.H., Stevens, T.J., Ferrante, R.J., Bird, E.D., and Richardson, E.P. (1985). Neuropathological classification of Huntington's disease. J. Neuropathol. Exp. Neurol. *44*, 559–577.

Wanker, E.E., Rovira, C., Scherzinger, E., Hasenbank, R., Walter, S., Tait, D., Colicelli, J., and Lehrach, H. (1997). HIP-1: a huntingtin interacting protein isolated by the yeast two-hybrid system. Human Mol. Genet. *6*, 487–495.

Wisden, W., Errington, M.L., Williams, S., Dunnett, S.B., Waters, C., Hancock, D., Evan, G., Bliss, T.V., and Hunt, S.P. (1990). Differential expression of immediate early genes in the hippocampus and spinal cord. Neuron *4*, 603–614.

Zeitlin, S., Liu, J.-P., Chapman, D.L., Papaioannou, V.E., and Estradiatis, A. (1995). Increased apoptosis and early embryonic lethality in mice nullizygous for the Huntington's disease gene homologue. Nature Genet. *11*, 155–163.